Human Quiescin-Sulfhydryl Oxidase, QSOX1: Probing Internal Redox Steps by Mutagenesis †

ARTICLE *in* BIOCHEMISTRY · APRIL 2008

Impact Factor: 3.02 · DOI: 10.1021/bi702522q · Source: PubMed

4 AUTHORS, INCLUDING:

Assaf Alon
Whitehead Institute for Biomedical Research
12 PUBLICATIONS **245** CITATIONS
SEE PROFILE

Colin Thorpe
University of Delaware
107 PUBLICATIONS **3,973** CITATIONS
SEE PROFILE

Human Quiescin-Sulfhydryl Oxidase, QSOX1: Probing Internal Redox Steps by Mutagenesis[†]

Erin J. Heckler,[‡] Assaf Alon,[§] Deborah Fass,[§] and Colin Thorpe*[,‡]

Department of Chemistry and Biochemistry, University of Delaware, Newark, Delaware 19716, and Weizmann Institute of Science, Rehovot, 76100 Israel

Received December 22, 2007; Revised Manuscript Received February 8, 2008

ABSTRACT: The flavoprotein quiescin-sulfhydryl oxidase (QSOX) rapidly inserts disulfide bonds into unfolded, reduced proteins with the concomitant reduction of oxygen to hydrogen peroxide. This study reports the first heterologous expression and enzymological characterization of a human QSOX1 isoform. Like QSOX isolated from avian egg white, recombinant HsQSOX1 is highly active toward reduced ribonuclease A (RNase) and dithiothreitol but shows a >100-fold lower k_{cat}/K_m for reduced glutathione. Previous studies on avian QSOX led to a model in which reducing equivalents were proposed to relay through the enzyme from the first thioredoxin domain (C70−C73) to a distal disulfide (C509−C512), then across the dimer interface to the FAD-proximal disulfide (C449−C452), and finally to the FAD. The present work shows that, unlike the native avian enzyme, HsQSOX1 is monomeric. The recombinant expression system enabled construction of the first cysteine mutants for mechanistic dissection of this enzyme family. Activity assays with mutant HsQSOX1 indicated that the conserved distal C509−C512 disulfide is dispensable for the oxidation of reduced RNase or dithiothreitol. The four other cysteine residues chosen for mutagenesis, C70, C73, C449, and C452, are all crucial for efficient oxidation of reduced RNase. C452, of the proximal disulfide, is shown to be the charge-transfer donor to the flavin ring of QSOX, and its partner, C449, is expected to be the interchange thiol, forming a mixed disulfide with C70 in the thioredoxin domain. These data demonstrate that all the internal redox steps occur within the same polypeptide chain of mammalian QSOX and commence with a direct interaction between the reduced thioredoxin domain and the proximal disulfide of the Erv/ALR domain.

All eukaryotic sulfhydryl oxidases yet described utilize either metal ions or a flavin cofactor to couple the oxidation of thiols with the reduction of oxygen to hydrogen peroxide:

$$2R{-}SH + O_2 \rightarrow R{-}S{-}S{-}R + H_2O_2$$

The copper- and iron-dependent enzymes are relatively poorly understood; there are no sequences, structures, or detailed analyses of the catalytic role of the metal (*1–4*). In contrast, a growing literature describes the structures, mechanisms, and roles in oxidative protein folding of the flavin-dependent sulfhydryl oxidases, *e.g.*, Ero1 and members of the Erv/ALR[1] family (4–11). The latter includes single-domain proteins, such as yeast Erv1p and Erv2p (*5–8*), mammalian augmenter of liver regeneration (ALR) (*9–11*), plant (*12, 13*) and viral (*14, 15*) sulfhydryl oxidases, and multidomain quiescin-sulfhydryl oxidases (QSOX) (*3, 4, 16, 17*), which are the subject of this contribution.

Rat seminal vesicle sulfhydryl oxidase, now known to be a member of the QSOX branch of the Erv/ALR family, was the first flavin-dependent sulfhydryl oxidase to be described (*18*). However most of the mechanistic work on these enzymes has utilized avian egg white QSOX (*2, 17, 19–21*). The initial anaerobic titrations of avian QSOX provided strong evidence for the presence of two redox centers: a flavin prosthetic group and a juxtaposed protein disulfide (*19*). This led to a proposal for the flow of reducing equivalents during QSOX catalysis (*21*):

$$\text{dithiol substrate} \rightarrow [\text{disulfide} \rightarrow \text{flavin}] \rightarrow \text{oxygen}$$

Although this minimal model (*19*) showed close parallels to that established for lipoamide dehydrogenase, glutathione reductase, and thioredoxin reductase (*22, 23*), QSOX enzymes were subsequently found to be evolutionarily unrelated to the pyridine nucleotide-disulfide oxidoreductase family (*24, 25*). In addition, the amino acid sequence and domain organization of avian QSOX (Figure 1) suggested the presence of additional potential redox-active disulfides that would have been spectroscopically silent in the initial series of anaerobic titrations (*17, 24*). The domain organization of metazoan QSOX from the amino terminus is as follows: two thioredoxin-like domains, a region predicted to be helix-rich (HRR) but about which little else is known, an Erv/ALR FAD-

[†] This work was supported in part by National Institutes of Health Grant GM26643 (C.T.) and the United States−Israel Binational Science Foundation (D.F.).

* Author for correspondence. Phone: (302) 831-2689. Fax: (302) 831-6335. E-mail: cthorpe@Udel.edu.

[‡] University of Delaware.

[§] Weizmann Institute of Science.

[1] Abbreviations: ALR, augmenter of liver regeneration; DTNB, 5,5′-dithiobis(2-nitrobenzoate); DTT, dithiothreitol; Erv/ALR, the family of enzymes that comprises homologues of the yeast protein "Essential for respiration and viability 1", including ALR; GSH, reduced glutathione; HRR, helix-rich region; IPTG, isopropyl-β-D-thiogalactopyranoside; PDI, protein disulfide isomerase; QSOX, flavin-dependent sulfhydryl oxidase homologous to quiescin Q6.

10.1021/bi702522q CCC: $40.75
Published on Web 04/05/2008

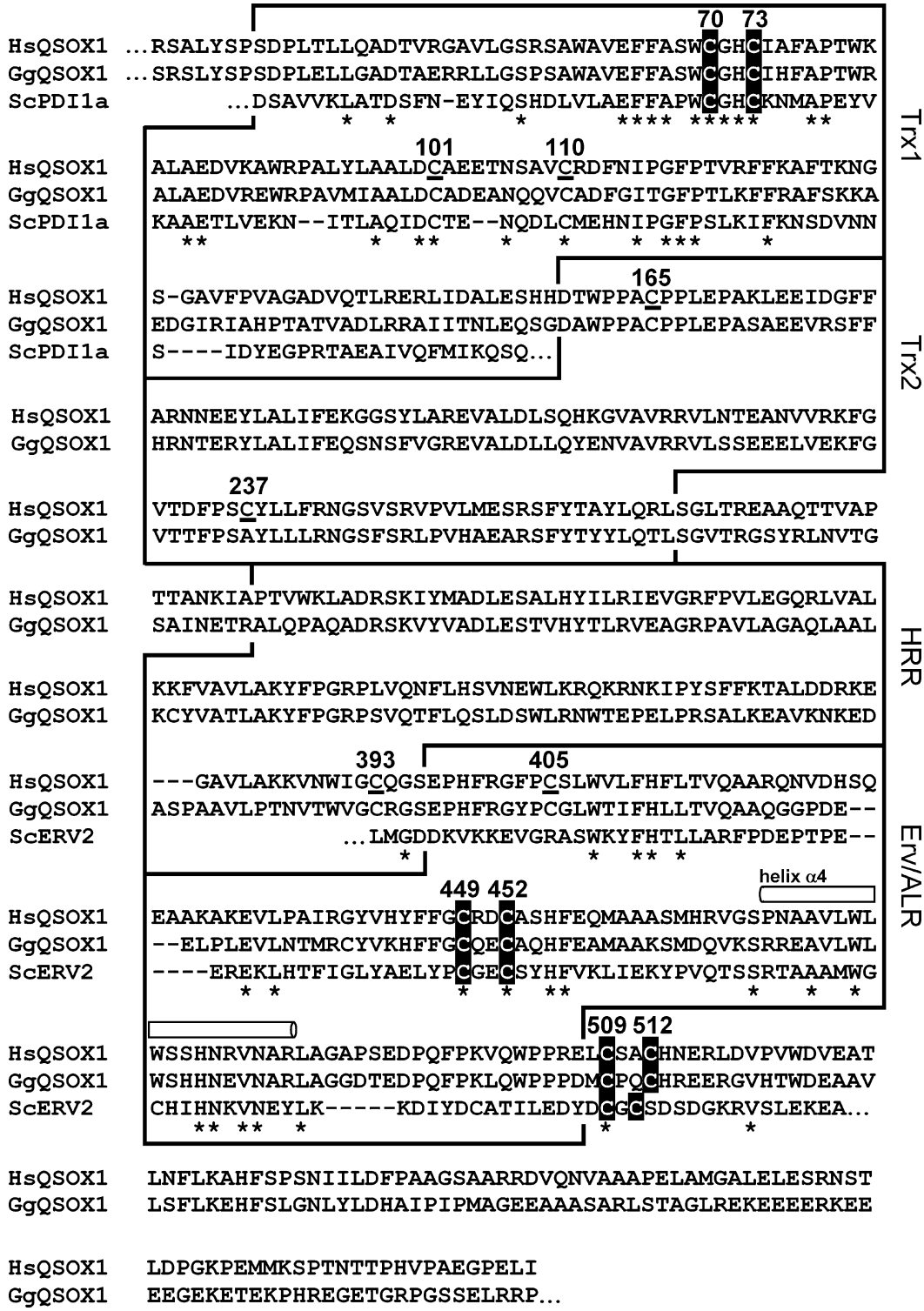

FIGURE 1: Domain organization of a metazoan QSOX and sequence comparisons with the "**a**" domain of yeast Pdi1p and yeast Erv2p. Partial sequences of human (HsQSOX1) and avian (GgQSOX1) enzymes are compared with an alignment to the "**a**" domain of yeast Pdi1p (ScPDI1a; NCBI Accession NP_009887.1) and the Erv/ALR domain of yeast Erv2p (ScErv2; NCBI Accession Q12284). The recognized domains of the short form of metazoan QSOX (Trx1, Trx2, HRR, and Erv/ALR) are boxed. Presumed redox active disulfides are shown in bold reverse type; the remaining six cysteines are underlined. Residues in human and avian QSOX1 that are conserved with the PDI1a or ScErv2 sequences are shown by the asterisks.

binding module (*7, 9, 13*), a region of high sequence variability predicted to be partially unstructured, and a membrane spanning region that can be eliminated by differential splicing to yield soluble isoforms (*3, 4, 25, 26*). The CxxC motif, common in proteins that undergo dithiol/disulfide redox reactions, is found in three places in the enzyme (*16, 17*): in the first thioredoxin-like domain (Trx1), in the Erv/ALR domain, and directly downstream of the Erv/ALR domain (Figure 1).

Two additional lines of evidence suggested that the initial mechanistic proposal was an oversimplification (*17*). Partial proteolysis of the avian oxidase showed that protein substrates of the enzyme interacted primarily with the CxxC motif of the Trx1 domain and that reducing equivalents were

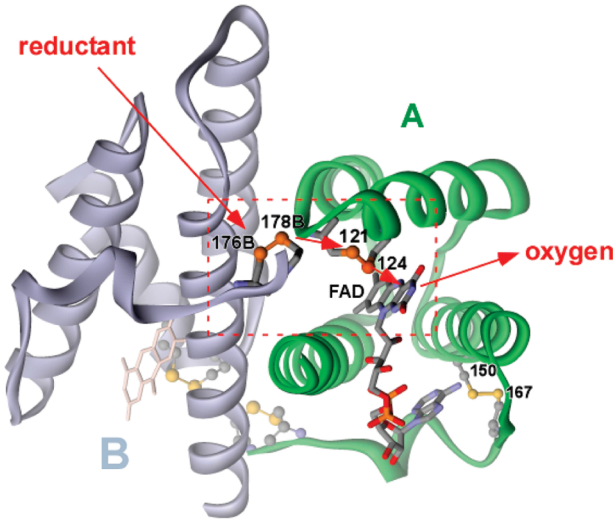

FIGURE 2: Crystal structure and the proposed flow of reducing equivalents in the yeast Erv2p homodimer. The proposed flow of reducing equivalents from the reductant (Pdi1p) to molecular oxygen is depicted from left to right using a series of arrows. An equivalent set of redox centers are shown unlabeled at the back of the homodimer. C150–167 is a structural disulfide in Erv2p that is absent in the multidomain quiescin-sulfhydryl oxidase (QSOX).

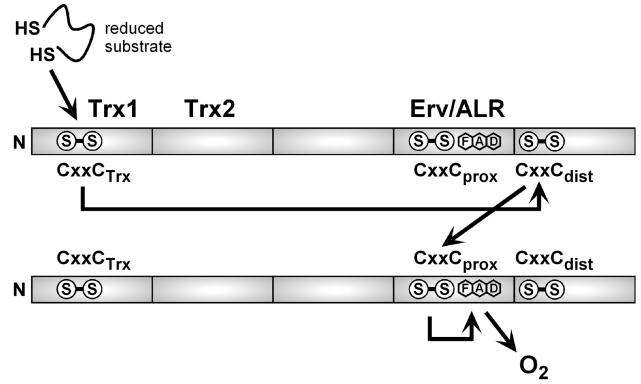

FIGURE 3: Suggested flow of reducing equivalents during oxidation of a reduced protein by avian QSOX1. The client reduced protein is oxidized by the Trx1 domain of QSOX followed by transfer of the pair of reducing equivalents to the Erv/ALR domain. The model incorporates an intersubunit disulfide exchange between distal and proximal CxxC motifs of a dimeric Erv/ALR domain as shown in Figure 2 (see text).

subsequently transferred between the Trx1 and Erv/ALR domains (*17*). Further insights were provided by the crystal structure of yeast Erv2p (*7*). Fass and co-workers proposed a model for the flow of reducing equivalents in this oxidase depicted in Figure 2 (*7*). The initial reduction of Erv2p occurs *via* dithiol/disulfide exchange with the distal (C176−C178) disulfide bond in one subunit of the homodimer (*7, 13, 27*). A second disulfide exchange across the dimer interface leads to the reduction of the proximal disulfide (C121−C124) in the opposite subunit followed by reduction of the flavin (*22, 28*) and transfer of reducing equivalents to molecular oxygen (*29, 30*). Single cysteine to alanine mutations of each of these four cysteine residues (C121, 124, 176, and 178) abolished the ability of Erv2p to rescue the growth defects of a yeast strain harboring a temperature-sensitive Ero1p mutant, consistent with an important role for shuttling reducing equivalents between distal and proximal disulfide/dithiol centers in dimeric Erv2p in vivo (*7*).

Several observations suggested (*17*) that avian QSOX had incorporated key aspects of the mechanism proposed for Erv2p. First, a distal CxxC motif is conserved in all available QSOX sequences (*16, 17*) and is located at a comparable position in the amino acid sequence to the CxC disulfide in yeast Erv2p (*7, 17*). If this distal disulfide were to occupy a position and play a role comparable to that depicted for Erv2p in Figure 2, then avian QSOX would be expected to be a dimer. Indeed both the full length egg white enzyme (*19*) and a proteolytic fragment containing the Erv/ALR domain (*17*) were found to be dimers by gel filtration. Finally, reductive titrations under forcing conditions showed that avian QSOX could accept a total of eight electrons (*17*), suggesting that the flavin and all three of the QSOX disulfides shown in Figure 3 (CxxC$_{Trx}$, CxxC$_{prox}$ and CxxC$_{dist}$) can undergo reduction. These data led Raje et al. to a more detailed model for avian QSOX catalysis (*17*) which utilized all three CxxC disulfides and an intersubunit transfer step as depicted in Figure 3.

Further progress in understanding the mechanism of QSOX enzymes required the application of site directed mutagenesis to study the individual roles of these six cysteine residues. We report here the first heterologous expression and enzymatic characterization of human QSOX1 and compare its catalytic specificity to the avian egg white and bovine milk proteins. Surprisingly, site-directed mutagenesis of the human enzyme demonstrates that it does not follow the catalytic mechanism shown in Figure 3. Our results, taken with complementary observations from smaller members of the Erv/ALR family of oxidases to be detailed later, show that monomeric versions of these enzymes can utilize a pathway for flow of reducing equivalents that bypasses the distal disulfide altogether. These studies provide important new insight into these intriguing catalysts of oxidative protein folding.

MATERIALS AND METHODS

Materials. Primers for the HsQSOX1b construct were from the Great American Gene Company, and primers for mutagenesis were from Integrated DNA Technologies. Ampicillin, tetracycline, chloramphenicol, riboflavin, protease inhibitor for His-tagged proteins, imidazole, RNase, catalase and glutathione were from Sigma. IPTG was from Promega; DTT was from Acros Organics; yeast, tryptone, NaCl, FAD, EDTA, and kanamycin sulfate were from Fisher.

Human QSOX1 Construct and Mutagenesis. Quiescin-sulfhydryl oxidase 1 (HsQSOX1) isoform b cDNA clone (ID 4447666) from human kidney mRNA was obtained from Invitrogen in the vector pCMV·SPORT6. The desired construct was amplified by PCR with an N-terminal forward primer omitting the signal sequence 5′-CTGGGATCCCG-GTCGGCGCTC-3′ (*Bam*HI site underlined) and a C-terminal reverse primer incorporating a stop codon, 5′-CTGAAGCTT*TCA*AATAAGCTC-3′ (stop codon italicized, *Hin*dIII site underlined). The construct was blunt-end ligated into a TOPO TA cloning vector pCR2.1 (Invitrogen) and digested with restriction enzymes. The insert was then ligated into the expression vector pTRC HisA (Invitrogen) digested with *Bam*HI and *Hin*dIII. This construct, including an N-terminal hexahistidine tag, was found to contain four sequence errors presumably as a result of low polymerase

fidelity. These errors were corrected by site-directed mutagenesis (QuikChange, Stratagene), and the construct was resequenced to ensure that no additional changes had been introduced. Site-directed cysteine mutations described in the text used the following primers: C70S, forward 5′-GCCTCCTGGAGCGGCCACTGCATCGCCTTCGCC-3′, reverse 5′-GGCGAAGGCGATGCAGTGGCCGCTCCAGGAGGC-3′; C73S, forward 5′-GCCTCCTGGTGCGGCCACAGCATCGCCTTCGCCCCGACGTGG-3′, reverse 5′-CCACGTCGGGGCGAAGGCGATGCTGTGGCCGCACCAGGAGGC-3′; C449A, forward 5′- GGCTACGTGCACTACTTCTTCGGCGCCCGAGACTGCGCTAGCCAC-3′, reverse 5′-GTGGCTAGCGCAGTCTCGGGCGCCGAAGAAGTAGTGCACGTAGCC-3′; C449S, forward 5′-GGCTACGTGCACTACTTCTTCGGCAGCCGAGACTGCGCTAGCCAC-3′, reverse 5′-GTGGCTAGCGCAGTCTCGGCTGCCGAAGAAGTAGTGCACGTAGCC-3′; C452S, forward 5′-GGCTGCCGAGACAGCGCTAGCCACTTCGAGCAG-3′, reverse 5′-CTGCTCGAAGTGGCTAGCGCTGTCTCGGCAGCC-3′; C509A, forward 5′-CCCCGTGAACTTGCTTCTGCCTGCCACAATGAACGC-3′, reverse 5′-GCGTTCATTGTGGCAGGCAGAAGCAAGTTCACGGGG-3′; C512A, forward 5′-CGTGAACTTTGTTCTGCCGCCCACAATGAACGC-3′, reverse 5′-GCGTTCATTGTGGGCGGCAGAACAAAGTTCACG-3′; C509SC512S, forward 5′-CCCCGTGAACTTAGTTCTGCCAGCCACAATGAACGCCGT-3′, reverse 5′-ACGGCGTTCATTGTGGCTGGCAGAACTAAGTTCACGGGG-3′. All constructs were fully sequenced to verify mutations and to ensure that no additional changes in the sequence had been introduced.

Expression of QSOX1 and Mutants. Expression of the QSOX1 construct in *Escherichia coli* was first attempted in BL21 DE3 cells (Invitrogen) at 37 °C. Cells were grown to an OD_{600} of 0.6 and then induced with 1 mM isopropyl-β-D-thiogalactopyranoside (IPTG) for 12 h. This resulted in the expression of mostly insoluble material. Autoinduction using BL21 (Star) DE3 cells was also assessed as a means of expressing HsQSOX1 but provided a low yield of soluble protein. Attempts to refold insoluble protein from inclusion bodies using 8 M guanidine hydrochloride in 100 mM DTT followed by dilution into a matrix of solutions from a Fold-It kit (Hampton Research) did not yield active protein.

The construct was then transformed into the Rosetta-gami DE3 strain (Novagen) that contains genes for rare tRNAs and mutations in the *trxB* (thioredoxin reductase) and *gor* (glutathione reductase) genes to enhance disulfide bond formation in the cytoplasm. A large number of expression trials with this construct (varying the times of growth and induction, the IPTG concentration, the temperature, and the use of rich and minimal growth media) were aimed at maximizing solubility and yield of protein. The following expression conditions gave workable, if low (~0.3 mg/L), purified yields of active HsQSOX1. Cultures were grown overnight at 37 °C in 5 mL of LB media supplemented with 50 μg/mL ampicillin, 34 μg/mL chloramphenicol, 15 μg/mL kanamycin, and 12.5 μg/mL tetracycline and used to inoculate four 2 L flasks each containing 500 mL of LB media supplemented with the same antibiotics and 5 μM riboflavin. Inoculated cultures were grown at 37 °C to OD_{600} 1.0–2.0. The cultures from the four flasks were then centrifuged and combined in fresh LB media supplemented as above and grown at 15 °C for 24 h in the presence of 0.2 mM IPTG. Cells were harvested at 5000*g* at 4 °C and stored at −20 °C before use.

Purification of QSOX1 and Mutants. Harvested cells were resuspended at 0.25 g of cell paste/mL of 50 mM potassium phosphate, pH 7.5, supplemented with 50 μM FAD, 0.1 mg/mL lysozyme, and a protease inhibitor cocktail for His-tagged proteins (Sigma: according to the manufacturer's instructions). The suspension was disrupted with two passes through a French press (10,000 psi) and clarified by centrifugation at 4 °C for 20 min at 8000*g*. The supernatant (20 mL) was added to 2 mL of Pro Bond Ni-NTA resin (Invitrogen) previously equilibrated in 50 mM potassium phosphate pH 7.5 containing 50 mM imidazole and 250 mM NaCl. The mixture was rocked overnight at 4 °C and packed into an empty column with elution of unbound materials. The resin was washed with three column volumes of 50 mM potassium phosphate pH 6.0 containing 1 M NaCl and 50 mM imidazole, followed by three column volumes of 50 mM potassium phosphate pH 7.5 containing 50 mM imidazole without NaCl. The column was developed with 5 mL of 100, 300, and 500 mM imidazole in 50 mM potassium phosphate pH 7.5. For wild-type QSOX1, the eluted protein fractions (at 300 mM imidazole) were purified using a second Ni-NTA column, incubating the protein solution with resin for one hour and using the same wash and elution steps. For QSOX1 mutants, the Ni-NTA column protein fractions were further purified on a Source 30 HR 5/5 cation exchange column using an AKTA FPLC (Amersham Pharmacia) with a 0–1 M NaCl gradient in 20 mM potassium phosphate pH 6.5, 1 mM EDTA. Following this second column purification, both wild-type and mutants were dialyzed against 50 mM potassium phosphate pH 7.5 containing 1 mM EDTA. Centrifuge ultrafiltration of recombinant human QSOX1, for protein concentration or buffer exchange, proved unsatisfactory because of aggregation at the membrane surface.

Size exclusion chromatography of the recombinant wild type enzyme was performed in 50 mM potassium phosphate pH 7.5 with 1 mM EDTA on a Superdex 200 HR 10/30 gel filtration column on the same FPLC system. The apparent native molecular weight of wild type recombinant enzyme was determined by comparison to a standard curve formed using thyroglobulin, ferritin, aldolase, bovine serum albumin, hemoglobin, chicken egg ovalbumin, and cytochrome *c*. Apparent molecular weights of the recombinant wild type and mutant enzymes were determined by 10% SDS−PAGE gels (Biorad) stained with Coomassie Blue.

UV/Vis Spectroscopy. Absorption spectra were obtained with an HP8453 instrument blanked with assay buffer 50 mM potassium phosphate pH 7.5 with 1 mM EDTA. Wild type enzyme concentrations were determined using an extinction coefficient for bound flavin of 12.5 mM^{-1} cm^{-1} at 456 nm (see below). The same extinction coefficient was used for all the mutants except the C449A and C449S mutants, which had extinction coefficients of 11.6 ± 0.4 mM^{-1} cm^{-1} and 11.2 ± 0.1 mM^{-1} cm^{-1} respectively at 456 nm. Scatter corrections were performed using the HP8453 Agilent ChemStation software.

Reduced RNase Assays. Reduced RNase was prepared by a modification of a prior procedure (*20*). Here, reduction was performed overnight at 4 °C and the protein was desalted on a PD10 column equilibrated with deoxygenated 0.1% v/v acetic acid. Reduced RNase was stored anaerobically and

standardized for thiol content prior to use (average of 8.0 DTNB-reactive thiols per RNase molecule). Sulfhydryl oxidase-mediated oxidation of RNase used the following concentrations: 35 μM to 1000 μM RNase thiols, 10 nM catalase, and 50 nM enzyme. Controls were run in the absence of enzyme. Samples were diluted 1:10 into 0.5 mM DTNB dissolved in 50 mM potassium phosphate pH 7.5, 1 mM EDTA and the thiol titer was recorded at 412 nm.

Oxygen Electrode Assays. Mutant and wild type oxidase activities were assayed in a Clark-type oxygen electrode as before (*19*). DTT was prepared in sample buffer and standardized with DTNB. Before standardization ~100 mM stock solutions of GSH in buffer were returned to pH 7.5 by the addition of concentrated KOH.

Extinction Coefficient Determination and Thiol Titer of HsQSOX1. The UV/vis spectrum of purified recombinant HsQSOX1 was recorded after dialysis into 100 mM Tris HCl pH 7.5, 1 mM EDTA and then remeasured 1 min after the addition of 0.1% SDS (from a 20% stock solution in water). Control experiments showed that the extinction coefficient of FAD (11.3 mM^{-1} cm^{-1}) was essentially unchanged in 0.1% SDS. The thiol titer of wild-type enzyme was determined after the addition of 0.5 mM DTNB to SDS-denatured protein.

Sequence Analysis and Modeling. DNA and amino acid sequence comparisons were done with LALIGN, ClustalW (*31*) and MultAlin (*32*) using default values. ClustalW and LALIGN were used to align the two thioredoxin domains of human QSOX1 against the sequence of the **a** and **b** domains of yeast Pdi1p ((*33*); PDB ID 2B5E) and of the oxidized and reduced forms of human thioredoxin 2 (PDB IDs 1W4V and 1W89, respectively). These alignments were submitted to SWISS-MODEL (*34*) and the resulting predictions viewed with Accelrys DS ViewerPro v5.0 and Swiss-Pdb viewer v3.7. MyHits Motif Scan (*35*) was used to help in domain boundary determination.

RESULTS AND DISCUSSION

Human QSOX1 Expression Construct: Domain Boundaries and Cysteine Content. Two transcripts of QSOX1 have been described, QSOX1a and -1b (*3, 4, 25, 26*). QSOX1a has a single transmembrane region, which is lacking in isoform 1b. In this study, the signal peptide of QSOX1b was replaced with a hexa-histidine tag followed by a 26 amino acid linker (Figure S2; Materials and Methods).

The twelve cysteines in the HsQSOX1 construct are listed in Table 1 and will be described in turn. The conserved CGHC motif in the Trx1 domain contains C70 and C73. A second cysteine pair (C101 and C110; Cx_8C, Figure 1) is conserved within the Trx1 domain in all of the metazoan and plant QSOX sequences so far examined but has a Cx_6C spacing in the *Trypanosoma* and *Leishmanii* QSOX proteins (Supporting Information, Figure S1). The cysteines in this $Cx_{6-8}C$ motif correspond to that of the Cx_6C disulfide bond found in the **a** domain of yeast Pdi1p (*33*). This particular disulfide (*33, 36–38*) has been suggested by Gilbert and coworkers (*38*) to play a regulatory role in Pdi1p by destabilizing the catalytic **a** domain disulfide. This presumed regulatory disulfide is encountered in Pdi1p homologues Eug1p (*39*) and Eps1p (*40*) and, with different spacings, in Mdp1p (Cx_8C (*41*)) and Mpd2p (Cx_7C (*42*)). The six-residue loop closed by the disulfide in yeast Pdi1p (*33*) might reasonably be expanded to eight residues in metazoan and plant QSOXs. The cysteines within the Trx2 domain, C165 and C237 (Figure 1), are not conserved (Supporting Information, Figure S1) and are unlikely to play a catalytic role. They are distant in sequence and appear 12–14 Å apart in homology models based on the yeast Pdi1p (PDB ID 2B5E) and human thioredoxin 2 (PDB ID 1W4V) structures. Close to the N-terminus of the Erv/ALR domain are the conserved C393 and C405 residues (Figure 1 and Supporting Information, Figure S1). Within the Erv/ALR domain are C449 and C452, which form the proximal CxxC disulfide, named for its predicted location next to the bound flavin. By analogy to the pyridine nucleotide disulfide oxidoreductase family (*22, 23*) and homology to Erv2p and ALR, C452 interacts primarily with the flavin. Its partner, C449, would then serve as the interchange cysteine, forming mixed disulfides with other redox centers. The final conserved cysteine pair, C509 and C512, is in a comparable position in the HsQSOX1 primary structure as the CxC motif of Erv2p and is expected to be in a flexible stretch of polypeptide chain prior to the beginning of the variable C-terminus.

Expression of Human QSOX1 in Escherichia coli. We used the *gor/trx* mutant *Escherichia coli* expression strain to produce HsQSOX1 because QSOX enzymes contain multiple disulfides. Induction at 37 °C led to expression of the protein as insoluble aggregates that could not be workably refolded using standard protocols. An increasing proportion of soluble enzyme was obtained as the induction temperature was lowered from 30 to 23 °C. However, the highest yields of active protein resulted from growth into log phase at 37 °C followed by resuspension of the cells in fresh media containing 0.2 mM IPTG and growth at 15 °C for 24 h. HsQSOX1 was purified from crude lysate by Ni-NTA chromatography, followed by application to a second Ni-NTA column for wild-type enzyme or to a Source 30 cation exchange column for mutant enzymes (see Materials and Methods). Typically, 0.3 mg of HsQSOX1 was obtained with >90% purity on SDS−PAGE from 1 L of the original 37 °C culture. Although yields are low, the enzyme is stable for several months when stored at 4 °C in 50 mM phosphate buffer pH 7.5, containing 1 mM EDTA. The modest levels of protein forced us to curtail some obvious approaches and to conduct spectrophotometric experiments in microcells to conserve material.

Recombinant HsQSOX1 was found to share many properties with the previously characterized QSOX enzymes. The UV–visible spectrum of recombinant HsQSOX1 shows a typical unresolved flavin envelope (Figure 4) that was seen for the rat seminal vesicle (RnQSOX1), the avian egg white (GgQSOX1) and the bovine milk (BtQSOX1) enzymes (*1, 18, 19*). The experimentally determined extinction coefficient is 12.5 ± 0.6 mM^{-1} cm^{-1} at 456 nm (see Materials and Methods), comparable to that obtained for GgQSOX1. HsQSOX1 contained 2.1 ± 0.1 DTNB-reactive thiols in denaturing conditions (see Materials and Methods), consistent with five disulfides and two free thiols. The apparent molecular weight of the enzyme on SDS−PAGE was 70 kDa, in good agreement with the expected value of 67.7 kDa from the sequence (Supporting Information, Figure S2). Gel filtration, using a calibrated size-exclusion column under nondenaturing conditions, gave a corresponding value of 76 kDa. The

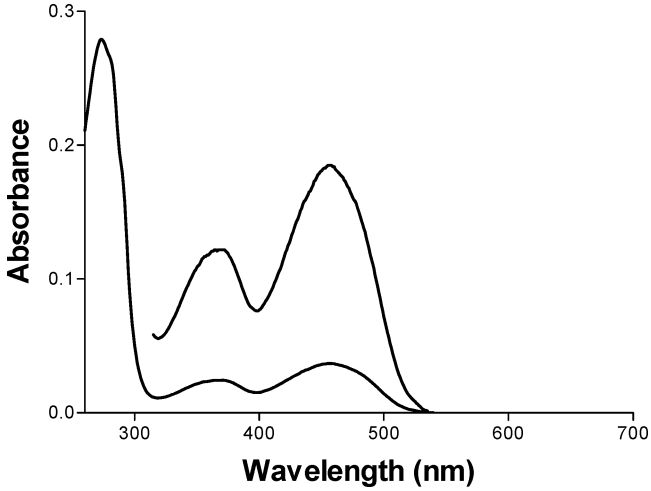

FIGURE 4: UV–visible spectrum of recombinant human QSOX1. The spectrum of 2.9 μM enzyme was recorded in 50 mM phosphate pH 7.5, containing 1 mM EDTA, and was corrected for small amounts of scattering material as described in Materials and Methods. The top spectrum is multiplied by 5 to show details of the flavin envelope.

striking result that recombinant HsQSOX1 is monomeric in solution was verified by equilibrium analytical ultracentrifugation (see Supporting Information, Figure S2).

Catalytic Activity of Recombinant HsQSOX1. Table 2 compares the catalytic activity of recombinant HsQSOX1 with native GgQSOX1 using three substrates: GSH, DTT, and RNase. As observed previously for GgQSOX1, reduced glutathione is a rather poor substrate of HsQSOX1 in terms of K_m (*19–21*). In contrast, reduced RNase is an excellent substrate of HsQSOX1, with catalytic efficiencies comparable to that observed with GgQSOX1 and BtQSOX1, consistent with the idea that reduced unfolded proteins may be the physiological substrates of this enzyme family (*4, 19–21*). We note that the K_m values for HsQSOX1, GgQSOX1, and BtQSOX1 toward GSH and DTT are comparable to those for the rat seminal vesicle enzyme described in 1980 (*18*). However the seminal vesicle enzyme is reported to have about 60- to 100-fold higher turnover numbers for GSH and DTT respectively (80,000 and 136,000 thiols oxidized per minute (*18*)). Our confidence in k_{cat} values in the 1000–4000/min range for vertebrate QSOXs (Table 2) is increased by our recent finding of similar values for native bovine QSOX1 (*1*). In summary, the recombinant human enzyme shows comparable activity to nonrecombinant avian and bovine QSOXs (Table 2).

Role of Three CxxC Motifs in HsQSOX1 Catalysis. The three CxxC motifs were previously implicated in catalysis of disulfide bond formation by GgQSOX1 (*2, 17*). To address the role of each CxxC motif in HsQSOX1, we made single Cys-to-Ala or -Ser mutants for all six cysteine residues; for one pair (509/512) we also generated an SxxS double mutant (see Materials and Methods). Activities of mutant proteins were initially measured using 5 mM DTT or 38 μM reduced RNase (0.3 mM thiols) as substrates (Table 3).

When cysteines in the CxxC motif of the HsQSOX Trx1 domain were mutated to serine (C70S and C73S), residual activities of about 7.5% of wild-type with DTT and 1.5% with reduced RNase were observed (Table 3). These activities likely represent the basal oxidase activity of the Erv/ALR domain. An Erv/ALR domain fragment of avian QSOX1 and several smaller sulfhydryl oxidases lacking Trx domains show turnover numbers from 20 to 150 thiols oxidized per min at 5 mM DTT and, correspondingly, 0–8/min toward reduced RNase (*6–8, 10, 17, 27, 43*).

We next mutated the two cysteine residues that comprise the proximal disulfide C449–452 in HsQSOX1 (corresponding to C121–124 in Erv2p; Figure 1). In Erv2p, C121, the residue furthest from the isoalloxazine ring, would correspond to the interchange thiol (following the nomenclature developed for the pyridine nucleotide disulfide oxidoreductases (*22, 23*) forming mixed disulfides with attacking thiolate nucleophiles. Scission of the proximal disulfide would then allow C124 to interact with the electron deficient isoalloxazine ring. Thiolate to flavin charge-transfer complexes have already been observed in static reductive titrations and during steady state turnover of avian QSOX1 (*19, 21*). Figure 5 confirms the identity of this charge-transfer donor as C452 as predicted from the sequence alignments and the structures of Erv/ALR family members (*7, 9, 44*). Thus, the spectrum of the C449A mutation shows a significant long wavelength feature centered at about 540 nm with the general signature of a charge-transfer interaction (*45, 46*). The C449S mutation also exhibits a long wavelength absorbance band but with a slightly different shape. While a serine residue may participate in hydrogen bonding interactions not found with alanine, a molecular explanation for this difference is not known at present. As expected the corresponding C452S mutation abolishes this charge-transfer interaction and leads to a native-like, but significantly blue-shifted, flavin envelope (Figure 5). Such blue shifts (here from 456 nm for the wild type to 449 nm) have been observed previously upon reduction of a disulfide adjacent to the flavin (*2, 17, 19, 47, 48*) and have been attributed to increased solvent access to the flavin that accompanies removal of the disulfide bond.

The C452S mutant shows very low activity with DTT and reduced RNase (0 and ~1% respectively; Table 3), as expected if this charge-transfer donor forms a covalent adduct with the flavin as a critical intermediate in the generation of dihydroflavin ((*22, 28*); Figure 6). While this adduct would normally be resolved by the interchange thiol (C449) as mentioned above, it might be attacked less effectively by one or more substrate thiols assuming the role of C449 in Figure 6. Thus the C449S mutant shows 4% and 2% of the wild type activity with DTT and reduced RNase, respectively (Table 3).

Surprisingly, mutations of the distal disulfide (C509–512, previously implicated in catalysis, see above) had comparatively minor effects on the turnover numbers observed with either 5 mM DTT or 300 μM reduced RNase thiols. Under these conditions the C509A mutant showed between 55 and 98% of the wild type activity and the corresponding C512A mutant between 26 and 59%. A double serine mutant retained 29–30% activity. These mutants were also evaluated by determining k_{cat} and K_m values for reduced RNase (Table 4). Again the impact of these mutations was minor, with k_{cat}/K_m values reduced by at most 4-fold (see later).

As mentioned earlier, the models for QSOX catalysis developed by analogy to Erv2p feature an intersubunit transfer of reducing equivalents from the distal (shuttle) to the proximal disulfides as depicted in Figures 1 and 3. However, we found that recombinant HsQSOX1 was monomeric. For example, gel filtration using a calibrated column

Table 1: Proposed Function and Connectivity of Cysteine Residues in Human QSOX1

cysteines	proposed connectivity	proposed function (domain location)	corresponding residues in related proteins
C70	disulfide, CxxC	catalytic (Trx1)	C61/C64, yeast PDI1p
C73			
C101	disulfide, Cx_8C	structural/regulatory (Trx1)	C90/C97, yeast PDI1p Cx_6C
C110			C91/C99, yeast Mpd2p Cx_7C
			C87/C96, yeast Mpd1p Cx_8C
C165	cysteines (not conserved)	(Trx2)	not applicable
C237			
C393	disulfide, $Cx_{11}C$	unknown (spacer-Erv/ALR interface)	spacer domain unique to QSOXs
C405			
C449	disulfide, CxxC	catalytic (Erv/ALR)	C121/C124, Erv2p
C452			
C509	disulfide, CxxC	uncertain, see text	C176/C178, Erv2p
C512		(Erv/ALR-C terminus interface)	

Table 2: Comparison of Substrate Kinetics for Human, Avian and Bovine QSOX1[a]

	human QSOX			avian QSOX[b]			bovine QSOX[c]		
	TN_{max}, min^{-1}	K_m, mM	TN_{max}/K_m, M^{-1} s^{-1}	TN_{max}, min^{-1}	Km, mM	TN_{max}/K_m, M^{-1} s^{-1}	TN_{max}, min^{-1}	K_m, mM	TN_{max}/K_m, M^{-1} s^{-1}
DTT	1240	0.10	2.0×10^5	2066	0.150	2.30×10^5	1880	0.086	3.66×10^5
GSH	1480	12.4	1.98×10^3	2770	20	2.30×10^3	1760	4.9	5.94×10^3
RNase	4320	0.32	2.2×10^5	1220	0.115	1.76×10^5	1340	0.060	3.74×10^5

[a] Turnover numbers are quoted in terms of thiols oxidized per min (and not disulfides generated per min as listed previously). [b] Taken from references to the avian (*19, 20*) and the bovine QSOX1 (*1*) enzymes expressing the turnover numbers as above. [c] Taken from references to the avian (*19, 20*) and the bovine QSOX1 (*1*) enzymes expressing the turnover numbers as above.

Table 3: Turnover Numbers for Wild-Type and Cysteine Mutants of HsQSOX1 Using DTT and Reduced RNase Substrates[a]

protein	5 mM DTT, TN min^{-1}	relative TN	300 μM RNase thiols, TN min^{-1}	relative TN
WT	1280 ± 40	1.00	2170 ± 14	1.00
C70S	88 ± 14	0.07	46 ± 24	0.02
C73S	108 ± 12	0.08	42 ± 16	0.02
C449S	48 ± 18	0.04	42 ± 20	0.02
C452S	0	0	16 ± 8	0.007
C509A	1260 ± 240	0.98	1200 ± 140	0.55
C512A	760 ± 10	0.59	570 ± 120	0.26
C509S,C512S	380 ± 60	0.30	630 ± 70	0.29

[a] Turnover numbers are reported as thiols oxidized (not disulfides generated) per minute.

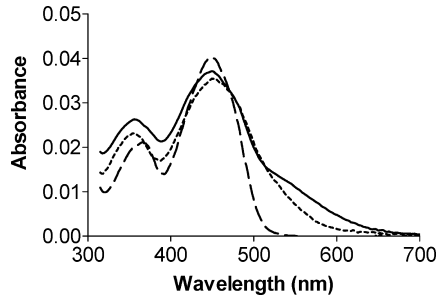

FIGURE 5: UV–visible spectra of cysteine mutants of the proximal disulfide of HsQSOX1. Spectra of the following mutants of HsQSOX1 in phosphate buffer pH 7.5: C449A (solid line), C449S (short dashed line), and C452S (long dashed line). Spectra were normalized to correspond to a concentration of 3.2 μM using the extinction coefficients reported in Materials and Methods.

gave an apparent molecular weight of 67 kDa (data not shown, see Materials and Methods). We also estimated the molecular weight by sedimentation equilibrium (see Supporting Information) as 70.7 kDa. Because the construct used for this study contained both an N-terminal His tag and a linker region of 26 amino acids, we also determined the molecular weight of a second construct of HsQSOX1 in which this extension to the N-terminus was removed (Supporting Information, Figure S4). This version also behaves as a monomer (Supporting Information, Figure S3). Thus the N-terminal His tag does not promote monomerization of a QSOX dimer. Consistent with these data, but in contrast to avian QSOX1 (*19*), rat seminal vesicle QSOX1 (*25*) and bovine QSOX1 (*1*) also elute as monomers on gel filtration (*18*). Finally the turnover number of HsQSOX1 with 5 mM DTT is unaffected over a 40-fold range of concentrations (from 5 to 200 nM QSOX; data not shown). Hence the active form of HsQSOX is a monomer under these conditions.

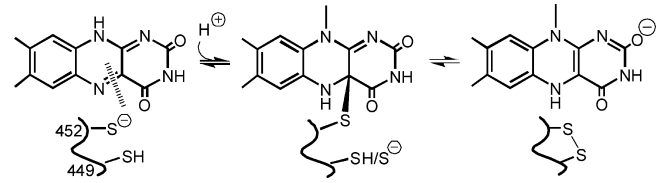

FIGURE 6: Proposed mechanism for the transfer of reducing equivalents between flavin and the reduced proximal disulfide in QSOX. The interchange and charge transfer thiols correspond to C449 and C452 respectively.

Table 4: Kinetic Parameters of Serine and Alanine Mutants of the Distal Disulfide

	RNase TN_{max}, min^{-1}	K_m, μM per thiol	TN_{max}/K_m, M^{-1} s^{-1}
WT	4320	320 ± 35	2.2×10^5
C509A	5240	700 ± 230	1.3×10^5
C512A	1680	420 ± 130	6.6×10^4
C509S,C512S	740	230 ± 20	5.4×10^4

CONCLUSIONS

Figure 7 presents a revised minimal catalytic mechanism for human QSOX1. We have shown that the HsQSOX1 monomer is active and that the conserved distal disulfide (*16*) does not have an essential role in catalysis of disulfide bond formation in dithiothreitol or reduced RNase. Distal disulfide mutants of HsQSOX1 show only small (up to

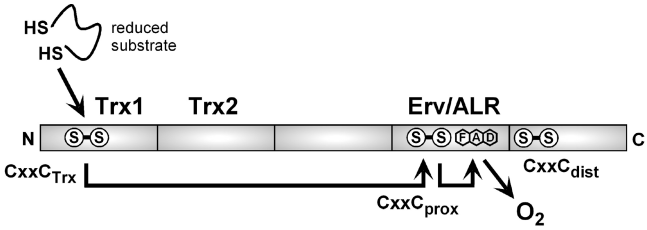

FIGURE 7: Revised model for flow of reducing equivalents in QSOX. This model involves a transitory mixed disulfide between C70 of Trx1 and C452 of the proximal disulfide in the Erv/ALR domain (see the text).

4-fold) decreases in k_{cat}/K_m in the oxidation of reduced RNase. It was observed previously that the distal disulfides of small Erv enzymes are also dispensable for certain activities. For example, Erv2p and AtErv1 lacking the distal disulfides oxidize DTT efficiently (*27*). More significantly, a monomeric mutant of Erv2p can oxidize model dithiol substrates and reduced Pdi1p without the obligatory intervention of the shuttle disulfide (*27*). This latter observation provides an important precedent in support of the model in Figure 7 in which a thioredoxin domain interacts directly with the proximal disulfide of a monomeric QSOX.

However, distal disulfides are essential for other activities of single-domain Erv/ALR sulfhydryl oxidases. For example, yeast strains expressing Erv2p without the distal disulfide no longer rescued a growth defect caused by the absence of functional Ero1p sulfhydryl oxidase (*7, 8*). In addition, the distal disulfide of an Erv/ALR sulfhydryl oxidase from *Arabidopsis thaliana* (AtErv1) was essential for the *in vitro* oxidation of reduced thioredoxin (*13*). From our experiments, we cannot exclude the possibility that the distal disulfide of QSOX is involved in an alternate pathway for the oxidation of protein substrates whose importance depends on the type of protein oxidized, or that the distal disulfide is involved in the regulation of enzyme activity. If the distal disulfide indeed participates in electron transfer from certain substrates to the FAD-proximal disulfide in monomeric HsQSOX1, then it must differ in position from the distal disulfides of small, dimeric Erv family enzymes. The striking divergence of the QSOX sequence from that of Erv2p after the end of the fourth helix in the bundle (Figure 1) prevents prediction of the position of the QSOX distal disulfide on the basis of the Erv2p structure and opens the possibility that it approaches within dithiol–disulfide exchange distance of the active-site disulfide on the same polypeptide chain.

Finally, we note interesting parallels between monomeric metazoan QSOXs and yeast PdiI1p. Both proteins have four principal domains with the outermost domains being the ones that carry redox-active CxxC motifs. QSOX requires intramolecular redox communication between the Trx1 domain and the Erv/ALR module, and, while interdomain transfer is not expected to be an essential feature of PDI catalysis, the two CxxC domains of PDI face each other across a flexible cavity formed from the four domains. This twisted U shaped cavity is lined with hydrophobic residues presumably to facilitate binding of protein substrates and to discourage their aggregation. It will be interesting to learn whether the hydrophobic surfaces of QSOXs (*19*) play a similar role in handling client proteins during oxidative protein folding.

ACKNOWLEDGMENT

We thank Steven G. Brohawn for early experiments on the expression of human QSOX1, and we thank members of our laboratories and an anonymous reviewer for their helpful comments.

SUPPORTING INFORMATION AVAILABLE

Figures S1–S4 show sequence alignments of selected QSOXs; the full sequence of the human QSOX1b construct used for most of this work; the sequence of the construct used for the analytical ultracentrifugation; and analysis of ultracentrifugation data. This material is available free of charge via the Internet at http://pubs.acs.org.

REFERENCES

1. Jaje, J., Wolcott, H. N., Fadugba, O., Cripps, D., Yang, A. J., Mather, I. H., and Thorpe, C. (2007) A flavin-dependent sulfhydryl oxidase in bovine milk. *Biochemistry 46*, 13031–13040.
2. Brohawn, S. G., Rudik, I., and Thorpe, C. (2003) Avian sulfhydryl oxidase is not a metalloenzyme: adventitious binding of divalent metal ions to the enzyme. *Biochemistry 42*, 11074–11082.
3. Thorpe, C., and Coppock, D. L. (2007) Generating disulfides in multicellular organisms: Emerging roles for a new flavoprotein family. *J. Biol. Chem. 282*, 13929–13933.
4. Coppock, D. L., and Thorpe, C. (2006) Multidomain flavin-dependent sulfhydryl oxidases. *Antioxid. Redox Signal. 8*, 300–311.
5. Lee, J., Hofhaus, G., and Lisowsky, T. (2000) Erv1p from Saccharomyces cerevisiae is a FAD-linked sulfhydryl oxidase. *FEBS Lett. 477* (1–2), 62–66.
6. Gerber, J., Muhlenhoff, U., Hofhaus, G., Lill, R., and Lisowsky, T. (2001) Yeast ERV2p is the first microsomal FAD-linked sulfhydryl oxidase of the Erv1p/Alrp protein family. *J. Biol. Chem. 276*, 23486–23491.
7. Gross, E., Sevier, C. S., Vala, A., Kaiser, C. A., and Fass, D. (2002) A new FAD-binding fold and intersubunit disulfide shuttle in the thiol oxidase Erv2p. *Nat. Struct. Biol. 9*, 61–67.
8. Sevier, C. S., Cuozzo, J. W., Vala, A., Aslund, F., and Kaiser, C. A. (2001) A flavoprotein oxidase defines a new endoplasmic reticulum pathway for biosynthetic disulphide bond formation. *Nat. Cell Biol. 3*, 874–882.
9. Wu, C. K., Dailey, T. A., Dailey, H. A., Wang, B. C., and Rose, J. P. (2003) The crystal structure of augmenter of liver regeneration: A mammalian FAD-dependent sulfhydryl oxidase. *Protein Sci. 12*, 1109–1118.
10. Farrell, S. R., and Thorpe, C. (2005) Augmenter of liver regeneration: a flavin dependent sulfhydryl oxidase with cytochrome C reductase activity. *Biochemistry 44*, 1532–1541.
11. Chen, X., Li, Y., Wei, K., Li, L., Liu, W., Zhu, Y., Qiu, Z., and He, F. (2003) The potentiation role of hepatopoietin on activator protein-1 is dependent on its sulfhydryl oxidase activity. *J. Biol. Chem. 278*, 49022–49030.
12. Levitan, A., Danon, A., and Lisowsky, T. (2004) Unique features of plant mitochondrial sulfhydryl oxidase. *J. Biol. Chem. 279*, 20002–20008.
13. Vitu, E., Bentzur, M., Lisowsky, T., Kaiser, C. A., and Fass, D. (2006) Gain of function in an ERV/ALR sulfhydryl oxidase by molecular engineering of the shuttle disulfide. *J. Mol. Biol. 362*, 89–101.
14. Senkevich, T. G., White, C. L., Koonin, E. V., and Moss, B. (2002) Complete pathway for protein disulfide bond formation encoded by poxviruses. *Proc. Natl. Acad. Sci. U.S.A. 99*, 6667–6672.
15. Rodriguez, I., Redrejo-Rodriguez, M., Rodriguez, J. M., Alejo, A., Salas, J., and Salas, M. L. (2006) African swine fever virus pB119L protein is a flavin adenine dinucleotide-linked sulfhydryl oxidase. *J. Virol. 80*, 3157–3166.
16. Heckler, E. J., Rancy, P. C., Kodali, V. K., and Thorpe, C. (2007) Generating disulfides with the quiescin sulfhydryl oxidases, Biochim. Biophys. Acta, Epub ahead of print.
17. Raje, S., and Thorpe, C. (2003) Inter-domain redox communication in flavoenzymes of the quiescin/sulfhydryl oxidase family: role of a thioredoxin domain in disulfide bond formation. *Biochemistry 42*, 4560–4568.

18. Ostrowski, M. C., and Kistler, W. S. (1980) Properties of a flavoprotein sulfhydryl oxidase from rat seminal vesicle secretion. *Biochemistry 19*, 2639–2645.
19. Hoober, K. L., Joneja, B., White, H. B., III, and Thorpe, C. (1996) A Sulfhydryl Oxidase from Chicken Egg White. *J. Biol. Chem. 271*, 30510–30516.
20. Hoober, K. L., Sheasley, S. S., Gilbert, H. F., and Thorpe, C. (1999) Sulfhydryl oxidase from egg white: a facile catalyst for disulfide bond formation in proteins and peptides. *J. Biol. Chem. 274*, 22147–22150.
21. Hoober, K. L., and Thorpe, C. (1999) Egg white sulfhydryl oxidase: Kinetic mechanism of the catalysis of disulfide bond formation. *Biochemistry 38*, 3211–3217.
22. Williams, C. H., Jr. (1992) in *Chemistry and Biochemistry of Flavoenzymes* (Müller, F., Ed.) pp 121–211, CRC Press, Boca Raton, FL.
23. Argyrou, A., and Blanchard, J. S. (2004) Flavoprotein disulfide reductases: advances in chemistry and function. *Prog. Nucleic Acid Res. Mol. Biol. 78*, 89–142.
24. Hoober, K. L., Glynn, N. M., Burnside, J., Coppock, D. L., and Thorpe, C. (1999) Homology between egg white sulfhydryl oxidase and quiescin Q6 defines a new class of flavin-linked sulfhydryl oxidases. *J. Biol. Chem. 274*, 31759–31762.
25. Benayoun, B., Esnard-Fève, A., Castella, S., Courty, Y., and Esnard, F. (2001) Rat seminal vesicle FAD-dependent sulfhydryl oxidase: biochemical characterization and molecular cloning of a member of the new sulfhydryl oxidase/quiescin Q6 gene family. *J. Biol. Chem. 276*, 13830–13837.
26. Thorpe, C., Hoober, K., Raje, S., Glynn, N., Burnside, J., Turi, G., and Coppock, D. (2002) Sulfhydryl oxidases: emerging catalysts of protein disulfide bond formation in eukaryotes. *Arch. Biochem. Biophys. 405*, 1–12.
27. Vala, A., Sevier, C. S., and Kaiser, C. A. (2005) Structural determinants of substrate access to the disulfide oxidase Erv2p. *J. Mol. Biol. 354*, 952–966.
28. Thorpe, C., and Williams, C. H. (1976) Spectral evidence for a flavin adduct in a monoalkylated derivative of pig heart lipoamide dehydrogenase. *J. Biol. Chem. 251*, 7726–7728.
29. Massey, V. (1994) Activation of molecular oxygen by flavins and flavoproteins. *J. Biol. Chem. 269*, 22459–22462.
30. Mattevi, A. (2006) To be or not to be an oxidase: challenging the oxygen reactivity of flavoenzymes. *Trends Biochem. Sci. 31*, 276–283.
31. Chenna, R., Sugawara, H., Koike, T., Lopez, R., Gibson, T. J., Higgins, D. G., and Thompson, J. D. (2003) Multiple sequence alignment with the Clustal series of programs. *Nucleic Acids Res. 31*, 3497–3500.
32. Corpet, F. (1988) Multiple sequence alignment with hierarchical clustering. *Nucleic Acids Res. 16*, 10881–10890.
33. Tian, G., Xiang, S., Noiva, R., Lennarz, W. J., and Schindelin, H. (2006) The crystal structure of yeast protein disulfide isomerase suggests cooperativity between its active sites. *Cell 124*, 61–73.
34. Schwede, T., Kopp, J., Guex, N., and Peitsch, M. C. (2003) SWISS-MODEL: An automated protein homology-modeling server. *Nucleic Acids Res. 31*, 3381–3385.
35. Pagni, M., Ioannidis, V., Cerutti, L., Zahn-Zabal, M., Jongeneel, C. V., and Falquet, L. (2004) MyHits: a new interactive resource for protein annotation and domain identification. *Nucleic Acids Res. 32*, W332–335.
36. Luz, J. M., and Lennarz, W. J. (1998) The nonactive site cysteine residues of yeast protein disulfide isomerase are not required for cell viability. *Biochem. Biophys. Res. Commun. 248*, 621–627.
37. Xiao, R., Wilkinson, B., Solovyov, A., Winther, J. R., Holmgren, A., Lundstrom-Ljung, J., and Gilbert, H. F. (2004) The contributions of protein disulfide isomerase and its homologues to oxidative protein folding in the yeast endoplasmic reticulum. *J. Biol. Chem. 279*, 49780–49786.
38. Wilkinson, B., Xiao, R., and Gilbert, H. F. (2005) A structural disulfide of yeast protein-disulfide isomerase destabilizes the active site disulfide of the N-terminal thioredoxin domain. *J. Biol. Chem. 280*, 11483–11487.
39. Tachibana, C., and Stevens, T. H. (1992) The yeast EUG1 gene encodes an endoplasmic reticulum protein that is functionally related to protein disulfide isomerase. *Mol. Cell. Biol. 12*, 4601–4611.
40. Wang, Q., and Chang, A. (1999) Eps1, a novel PDI-related protein involved in ER quality control in yeast. *EMBO J. 18*, 5972–5982.
41. Tachikawa, H., Takeuchi, Y., Funahashi, W., Miura, T., Gao, X. D., Fujimoto, D., Mizunaga, T., and Onodera, K. (1995) Isolation and characterization of a yeast gene, MPD1, the overexpression of which suppresses inviability caused by protein disulfide isomerase depletion. *FEBS Lett. 369*, 212–216.
42. Tachikawa, H., Funahashi, W., Takeuchi, Y., Nakanishi, H., Nishihara, R., Katoh, S., Gao, X. D., Mizunaga, T., and Fujimoto, D. (1997) Overproduction of Mpd2p suppresses the lethality of protein disulfide isomerase depletion in a CXXC sequence dependent manner. *Biochem. Biophys. Res. Commun. 239*, 710–714.
43. Wang, W., Winther, J. R., and Thorpe, C. (2007) Erv2p: characterization of the redox behavior of a yeast sulfhydryl oxidase. *Biochemistry 46*, 3246–3254.
44. Hofhaus, G., Lee, J. E., Tews, I., Rosenberg, B., and Lisowsky, T. (2003) The N-terminal cysteine pair of yeast sulfhydryl oxidase Erv1p is essential for in vivo activity and interacts with the primary redox centre. *Eur. J. Biochem. 270*, 1528–1535.
45. Abramovitz, A. S., and Massey, V. (1976) Interaction of phenols with old yellow enzyme. Physical evidence for charge-transfer complexes. *J. Biol. Chem. 251*, 5327–5336.
46. Massey, V., and Ghisla, S. (1974) Role of charge-transfer interactions in flavoprotein catalysis. *Ann. N.Y. Acad. Sci. 227*, 446–465.
47. Thorpe, C., and Williams, C. H., Jr. (1976) Differential reactivity of the two active site cysteine residues generated on reduction of pig heart lipoamide dehydrogenase. *J. Biol. Chem. 251*, 3553–3557.
48. Wilkinson, K. D., and Williams, C. H., Jr. (1979) Evidence for multiple electronic forms of two-electron-reduced lipoamide dehydrogenase from Escherichia coli. *J. Biol. Chem. 254*, 852–862.

BI702522Q